neuroectodermal markers such as NESTIN and SOX1 [32] were similar (Fig. 4A). In contrast, LDN treatment had no effect on the expression levels of differentiation markers in control iPSC line (Fig. 4A). We also found that the expression levels of markers found to be elevated in FOP-derived iPSC lines not treated with LDN are enhanced by BMP-4 stimulation in control iPSC lines (supporting information Fig. S5). We performed principal component analysis (PCA) [36] and hierarchical clustering of all genes to determine overall differences in transcription levels between FOP-derived iPSC lines and control iPSC lines (Fig. 4B, 4C). We added the datasets for 201B7, normal iPSC line, and three ESC lines from Gene Expression Omnibus datasets, GSE29115, GSE22167, and GSE37258 into our analyses. The gene-expression profile of FOP-derived iPSC lines not treated with LDN was distinct from that of control iPSC lines and those treated with LDN. In contrast, the gene-expression profile of FOP-derived iPSC lines treated with LDN was grouped closely to control iPSC lines not treated with LDN as did normal iPSC lines (N3-1 and DiPS) treated with LDN.

As shown in Figure 4C, each dataset for 201B7 and three ESC lines are separated from that for normal iPSC lines (N3-1 and DiPS) and FOP-iPSCs. In PCA analysis (Fig. 4B), the datasets for iPSC (red group) are broadly varied in the *y*-axis (PC3) direction compared with fibroblast datasets (yellow group). Therefore, the separation seen in the cluster analysis may reflect the above-mentioned differences, and such differences are thought to depend on the methods of iPSC induction (between retrovirus and SeV) and/or those between ESCs and iPSCs.

Comparing each gene-expression profile of FOP-derived iPSC lines treated with LDN to those not treated with LDN revealed upregulated and downregulated genes with a fold change of >2. Overall, with these datasets combined, we identified 526 commonly upregulated and 131 commonly downregulated genes (Fig. 4D). In addition, gene ontology analysis revealed that the molecular signature related to development and differentiation was frequently detected in commonly upregulated genes (Fig. 4E). In contrast, no specific signature was found in downregulated genes with a *p*-value cutoff of .1. Taken together, these results suggest that constitutive activation of ALK2 can promote the differentiation of iPSCs.

Efficient iPSC Generation Requires ALK2 Inhibitor Treatment Within an Optimal Time Frame

To further explore the effect of constitutive activation of ALK2 on iPSC generation, we investigated the time frame of inhibition of iPSC generation by the ALK2 mutant. We treated cultures with the ALK2 inhibitor for various periods of time and then counted the number of AP-positive (AP^+) colonies on day 30 after exposure (Fig. 5A). The highest number of AP^+ colonies was detected when FOP-derived fibroblasts were treated with the inhibitor from day 8 to day 30 (Fig. 5B, 5C). Treatment from day 1 to day 30 gave a lower level of efficiency. Furthermore, colony-forming efficiency was not restored by treating iPSC-induction cultures from day 1 to day 7 only. To further examine the period from day 8 to day 30, we counted the number of AP^+ colonies from day 8 to day 14, from day 15 to day 21, and from day 22 to day 30 (Fig. 5A, 5C). Unexpectedly, we counted few AP^+ colonies in every period. Taken together, these results suggested that the formation of iPSC colonies from FOP fibroblasts requires the inhibition of mutant ALK2 activity from day 8 to day 30 of iPSC induction and not during the early phase from day 1 to day 7.

Constitutive Activation of ALK2 in FOP Fibroblasts Inhibits Cellular Reprogramming

To elucidate the mechanisms underlying the inhibition of iPSC generation from FOP fibroblasts, we investigated whether the ALK2 mutation in FOP affects cellular reprogramming. We noticed that Tra-1-60, a pluripotency marker expressed on the iPSC surface, appeared during the early phase ($\sim$ day 7) of iPSC induction (Fig. 6A). Expression of Tra-1-60 was reduced on day 14 but then was markedly increased again up to day 21. The proportion of Tra-1-60^+ cells was lower in cultures of FOP-derived fibroblasts undergoing iPSC induction than in cultures of control fibroblast (Fig. 6A). However, Tra-1-60 expression was restored on day 21 in cultures treated with LDN. Consistent with this result, BMP-4 treatment inhibited the expression of Tra-1-60 during iPSC generation (Fig. 6A). To confirm that suppression of Tra-1-60 expression is due to the ALK2 mutation, we generated a shRNA expression construct specific for the ALK2 mutant R206H (Fig. 6B). The reporter plasmids are constructed by inserting synthetic oligonucleotides of normal and mutant ALK2 *allelic* sequence into 3′UTR of each luciferase genes [37]. The activity of luciferase carrying mutant ALK2 *allelic* sequence was specifically suppressed by shRNA expression (Fig. 6B). This shRNA effectively suppressed expression of the ALK2 mutant in FOP-derived fibroblasts and restored Tra-1-60 expression to control levels (Fig. 6C, 6D). Consistently, the generation of iPSC was partially improved by shRNA expression (supporting information Fig. S6A). Taken

Figure 4. Characterization of fibrodysplasia ossificans progressive (FOP)-derived iPSCs. **(A):** Global gene-expression patterns of normal and FOP-derived iPSCs. Scattered plot representation of the global gene-expression patterns for the iPSC lines N3-1, F1-1, F2-1, and F4-1 in the presence and absence of LDN-193189 (LDN) were compared. N3-1: Normal iPSC line; F1-1, F2-2, and F4-1: FOP-derived iPSC lines. **(B):** Principal component analysis. All datasets were classified into three principal components; PC1 (53.17%), PC2 (32.59%), and PC3 (14.23%) and were simplified into three-dimensional scores. Percentage shows the portion of variance in each component. The position of fibroblasts (yellow group) and normal- and FOP-derived iPSCs (red and blue groups) are clearly separated. The position of FOP-derived iPSC lines without LDN treatment (blue group) is further separated from that of control iPSC and embryonic stem cell (ESC) lines (red group). FOP-derived iPSC lines with LDN treatment are closely positioned to normal iPSC lines (N3-1 and DiPS) and human ESC lines referred for Gene Expression Omnibus datasets, GSE29115, GSE22167, and GSE37258. **(C):** Hierarchical clustering of all genes. The datasets of all genes investigated were clustered according to Euclidean distance metrics. Then, the datasets of fibroblasts and those of iPSC lines were classified into separate branches (yellow vs. red and blue). Furthermore, FOP-derived iPSC lines with LDN treatment were close to that of normal iPSC lines (N3-1 and DiPS) with or without LDN treatment. In contrast, FOP-derived iPSC lines without LDN treatment were classified into different branches from those of normal iPSC and ESC lines and FOP-derived iPSC lines treated with LDN (red vs. blue). **(D):** Venn diagram for the genes that were upregulated or downregulated by twofold or more between FOP-derived iPSC lines with or without LDN treatment. Comparing upregulated or downregulated gene profiles between FOP-derived iPSC lines with and without LDN treatments, the expression of 526 genes was shown to be commonly upregulated and those of 131 genes was shown to be downregulated. **(E):** Gene ontology (GO) analysis of commonly upregulated 526 genes. The top thirty-three of GO terms (percentage count are more than 5%) are listed. GO terms related to development and differentiation were frequently detected (underlines). Among the downregulated 131 genes, no GO terms were detected with a cutoff *p*-value of .1. Values are percentage count in all genes. Abbreviations: iPS, induced pluripotent stem; LDN, LDN-193189.

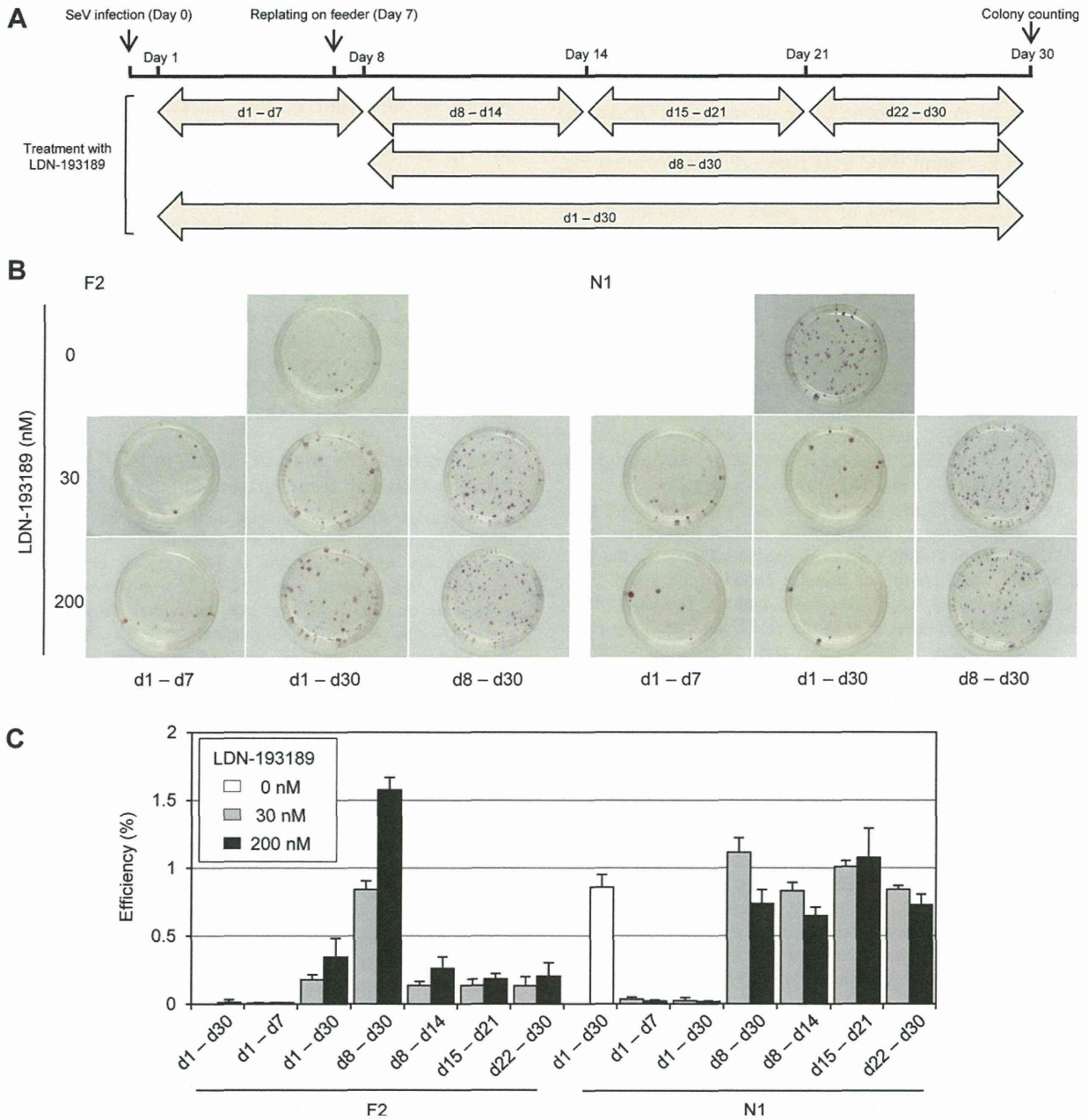

Figure 5. Efficient generation of induced pluripotent stem cells (iPSCs) from fibrodysplasia ossificans progressive (FOP)-derived fibroblasts during the time frame of activin receptor-like kinase 2 (ALK2) inhibition. **(A):** Experimental design for determination of the time frame of ALK2 inhibition. FOP-derived fibroblast cultures for the induction of iPSCs were treated with LDN for the indicated periods. **(B):** Alkaline phosphatase (AP) staining of iPSC colonies from patient F2 (left) and healthy volunteer N1 (right). Colonies in 60 mm dishes were treated with LDN at 0 nM, 30 nM, and 200 nM for the indicated periods (day 1–day 7 [d1–d7], day 1–day 30 [d1–d30], and day 8–day 30 [d8–d30]). **(C):** Efficiency of formation of iPSC colonies from FOP-derived fibroblasts treated with LDN for the indicated periods. AP^+ colony with undifferentiated colony morphology was counted as a typical colony on day 30. Abbreviations: LDN, LDN-193189; SeV, Sendai virus.

together, these results demonstrate that the suppression of Tra-1-60^+ cell generation is due to the mutant ALK2 in FOP.

To further evaluate the reprogramming status of the fibroblasts, we purified Tra-1-60^+ and Tra-1-60^- cells from day 7 cultures by fluorescence-activated cell sorting and investigated the expression of other pluripotent and fibroblastic markers. Fibroblastic markers, such as PDGFRα and VIMENTIN, which are strongly expressed in fibroblasts, should be downregulated during iPSC generation because they are not expressed in iPSCs. The endogenous genes OCT3/4 and NANOG are expressed in day 7 Tra-1-60^+ cells but not in day 7 Tra-1-60^- cells in both control and FOP-derived cultures (Fig. 6E). The expression levels of these pluripotent markers are significantly lower in FOP-derived Tra-1-60^+ cells than in controls. There was no expression of SOX2, REX1, KLF5, or DNMT3b in neither Tra-1-60^+ nor Tra-1-60^- cells (supporting information Fig. S6B). The expression of fibroblastic markers was downregulated in Tra-1-60^+ cells. However, the expression levels of PDGFRα and β and VIMENTIN were significantly higher in FOP-derived Tra-1-60^+ cells than in controls (Fig. 6F). These results suggest that the reprogramming status of FOP fibroblasts is incomplete,

despite the appearance of pluripotency marker expression in these cells.

The inhibition of ALK2 by LDN during the later phase of iPSC induction can recover the colony-forming capacity of iPSCs. This finding suggests that newly generated iPSCs cannot be maintained due to the constitutive activation of mutant ALK2 in FOP-derived fibroblasts and that as a result iPS colonies cannot form. To prove this hypothesis, we investigated the effect of BMP signaling on the colony-forming capacity of iPSCs. We showed that BMP-4 and BMP-7 treatments

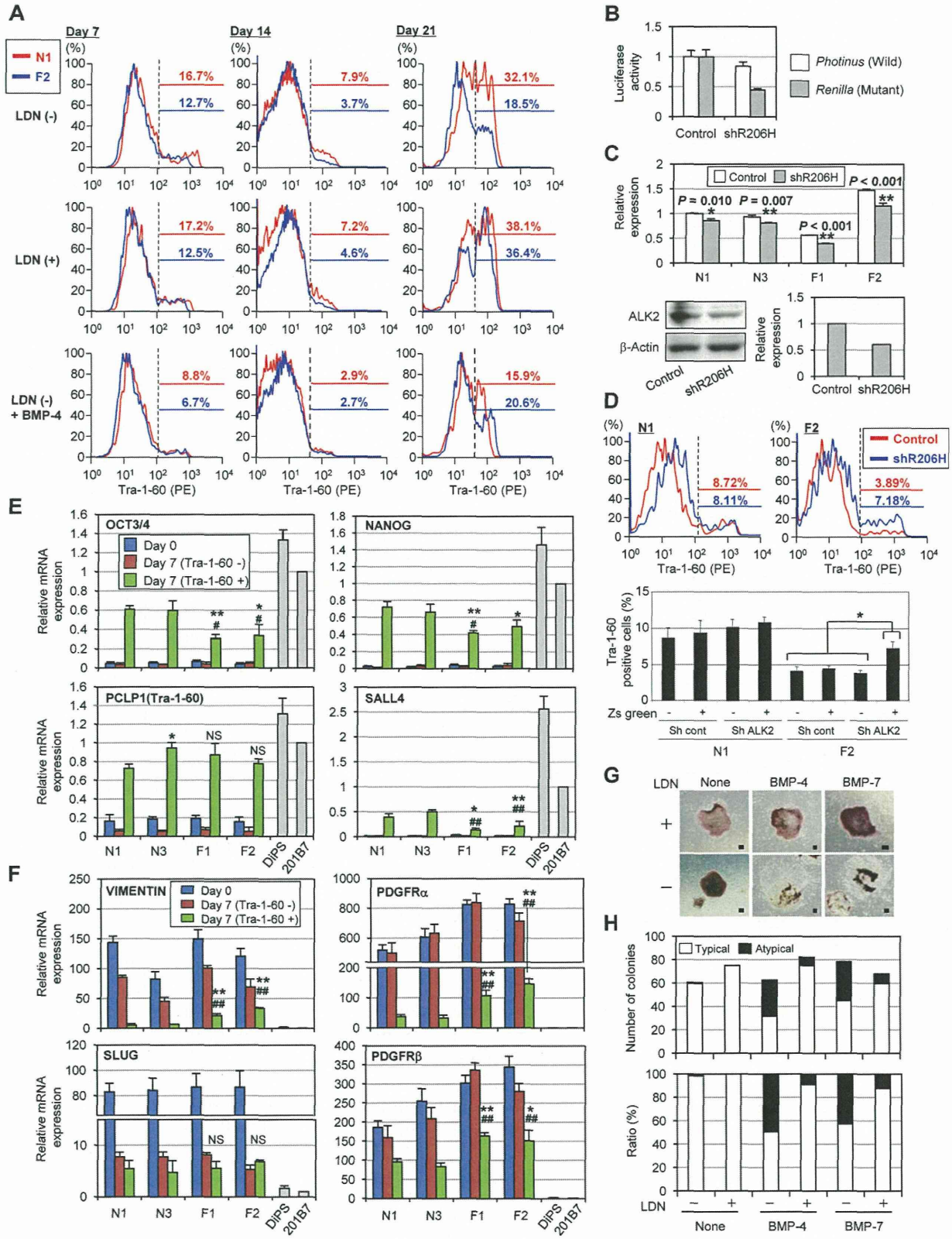

Figure 6. (legend on page 2446).

reduced the area of AP^+ cells in each iPSC colony (Fig. 6G). Morphological analysis revealed that this enforced BMP signaling disrupts the formation of iPSC colonies (Fig. 6G, 6H). Given the fact that BMP signals can induce the differentiation of iPSCs, these results suggest the existence of at least the two distinct mechanisms underlying the inhibition of iPSC generation; the first is incomplete reprogramming of pluripotent and fibroblastic genes, and the second is the forced differentiation of the cells during and after reprogramming.

Previous studies demonstrated that TGF-β/Activin signals affect iPSC generation [38]. Smad2 and 3, the downstream molecules of TGF-β/Activin receptors, are phosphorylated by the activation of these signals. However, we could not detect any change in Smad2 and 3 phosphorylations between normal and FOP-derived fibroblasts, suggesting that ALK2 mutation observed in FOP does not affect TGF-β/Activin signals during iPSC generation (supporting information Fig. S6C--S6F).

Inhibited Production and Maintenance of FOP-derived iPSC is a Useful Phenotype for Identifying Drug Candidates for Future Therapies

Our observation that treatment of FOP-derived fibroblasts with an ALK2 inhibitor allows iPSCs to be generated and maintained with pluripotency prompted us to use this system to identify candidate ALK2 inhibitors. We performed in silico screening by the multidirectional similarity search system and collected 160 bioactive compounds (see Materials and Methods). Our screen of the chemical library resulted in the identification of new candidate ALK2 inhibitors. One of them, RK-0071142 suppressed Smad1/5/8 phosphorylation (Fig. 7A, 7B). We used a cell-based assay of BMP signaling to show that the half-maximal inhibitory concentration (IC_{50}) of RK-0071142 was 1.44 μM for BMP-6 and 4.08 μM for BMP-4 (Fig. 7C and supporting information Fig. S7). Treatment of FOP-derived fibroblasts with RK-0071142 restored their capacity to generate iPSCs but with efficiency lower than that of LDN (Fig. 7D). The spontaneous differentiation of FOP-derived iPSCs was suppressed by RK-0071142 at a similar level to that of LDN (Fig. 7E). These results, together with LDN analyses, indicate that the generation and maintenance of FOP-derived iPSCs is a useful system for evaluating the bioactivity of new candidates as ALK2 inhibitors.

Discussion

In this study, we demonstrated that constitutive activation of ALK2 inhibits the generation and maintenance of human iPSCs. We also show that two distinct mechanisms underlie the inhibition of iPSC generation, the incomplete reprogramming of pluripotent and fibroblastic genes, and the forced differentiation of the cells during and after reprogramming.

Mutations in ALK2 underlie phenotypic variations of FOP and confer constitutive activity to the mutant receptor [3–9]. ALK2 acts as a type I receptor of BMPs, which are members of the TGF-β family [39]. TGF-βs and their family members are implicated in the generation and maintenance of iPSCs. Activation of TGF-β signaling blocks the cellular reprogramming required for the differentiation of a somatic cell into a pluripotent one and thus results in a reduction in the efficiency of iPSC generation [38]. Consistently, the blocking of TGF-β signaling by inhibiting ALK5 kinase, which is a receptor of TGF-β, augments the formation of iPSC colonies [40]. In contrast, a recent study using MEFs demonstrated that BMP signaling during the early-stage of iPSC induction ($\sim$ day 8) can enhance the generation of iPSCs. This signal induces a set of miRNAs associated with the mesenchymal-to-epithelial transition (MET), which can accelerate the generation of iPSCs [41]. BMP signaling occurs via a tetrameric complex of two out of three type II receptors, namely, BMP receptor II (BMPRII), activin receptor type II (ActRII), and ActRIIB; and two out of three BMP type I receptors, namely, ALK2, 3, and 6 [42]. Suppression of BMPRII and ALK3 inhibits the

Figure 6. Inhibitory mechanism of induced pluripotent stem cell (iPSC) generation from fibrodysplasia ossificans progressive (FOP)-derived fibroblasts. **(A):** Tra-1-60 expression during iPSC generation. After Sendai virus infection, the fibroblasts derived from FOP patients and healthy controls were cultivated without LDN [LDN(−)], with LDN [LDN(+)], and without LDN in the presence of BMP-4 [LDN(−) + BMP-4]. The expression of Tra-1-60, a pluripotency surface marker, was analyzed by fluorescence-activated cell sorting (FACS) on day 7, day 14, and day 21 of the iPSC induction period. Red line: expression pattern of healthy control (N1). Blue line: expression pattern of FOP (F2). **(B):** Assessment of specific inhibition of mutant activin receptor-like kinase 2 (ALK2) by shR206H. The silencing effect of shR206H was examined by luciferase and β-galactosidase assays. The expression levels of the *Photinus* (Wild) and *Renilla* (Mutant) luciferases and β-galactosidase were measured, respectively. The levels of both mutant and wild-type luciferase reporter allele activities were normalized to β-galactosidase activity. Values are average of four independent determinations. The ratios of the mutant and normal reporter activities in the present of shR206H were normalized to the control ratio obtained in the presence of the pSIREN-RetroQ-ZsGreen control plasmid. Error bars represent standard deviations. **(C):** Expression of ALK2 in FOP-derived fibroblasts treated with shRNA. The quantitative RT-PCR (qRT-PCR) analysis revealed that expression of ALK2 mRNA is significantly reduced by shRNA treatment (upper panel). Suppression of ALK2 expression was also confirmed by immunoblot analysis (lower panel). The data are means ± SD of triplicated cultures. Unpaired Student's *t* test was performed to evaluate differences between two groups. *, $p < .05$; **, $p < .01$, when compared with the values of respective control. **(D):** Treatment with shRNA specific for the ALK2 mutant R206H can restore expression of Tra-1-60. Virus carrying shRNA and ZsGreen cDNA was infected into both normal and FOP-derived fibroblasts. Tra-1-60 expression of $ZsGreen^+$ cells is measured by FACS. The representative data are shown in the upper panel. The results are summarized in the lower graph. It is significantly recovered to normal level by treatment with the shRNA. *, $p < .05$. **(E):** Expression of pluripotent signature genes. On day 7 of iPSC induction, Tra-1-60^+ and Tra-1-60^- cells were purified by FACS and the expression of endogenous genes related to pluripotency was then measured by qRT-PCR. The expression of OCT3/4, NANOG, and SALL4 was exclusively detected in Tra-1-60^+ cells but was significantly lower in FOP-derived Tra-1-60^+ cells than in normals. PCLP1 encodes Tra-1-60. The data are means ± SD of three independent experiments. A one-way ANOVA followed by Tukey's multiple comparison test was performed to evaluate differences between groups. *, $p < .05$, **, $p < .01$, when compared with the values of day 7 (Tra-1-60^+) from fibroblast N1. $^{\#}$, $p < .05$, $^{\#\#}$, $p < .01$, when compared with the values of day 7 (Tra-1-60^+) from fibroblast N3. **(F):** Incomplete reprogramming of fibroblastic markers. After Tra-1-60^+ and Tra-1-60^- cells were purified by FACS on day 7 of iPSC induction, the expression of fibroblastic markers was measured by qRT-PCR. The expression of PDGFRα and VIMENTIN of FOP-derived Tra-1-60^+ cells was significantly higher than that of control Tra-1-60^+ cells, suggesting that these genes are insufficiently downregulated during iPSC generation from FOP fibroblasts. The statistical analysis is described in (E). **(G, H):** BMPs can inhibit the colony formation of iPSCs during their induction. Colony morphology of iPSCs with alkaline phosphatase staining (G) and the number and percentage of typical and atypical iPSC colonies with or without BMP treatment (H). Almost all colonies are typical in cultures without BMPs or with both BMPs and LDN. In contrast, 50% of the colonies was atypical in cultures treated with BMPs. The concentrations of BMP-4 and BMP-7 are 10 ng/ml and 25 ng/ml, respectively. Typical and atypical colonies are defined as shown in Figure 1D. Scale bars = 200 μm. Abbreviations: BMP, bone morphogenetic protein; LDN, LDN-193189; NS, not significant.

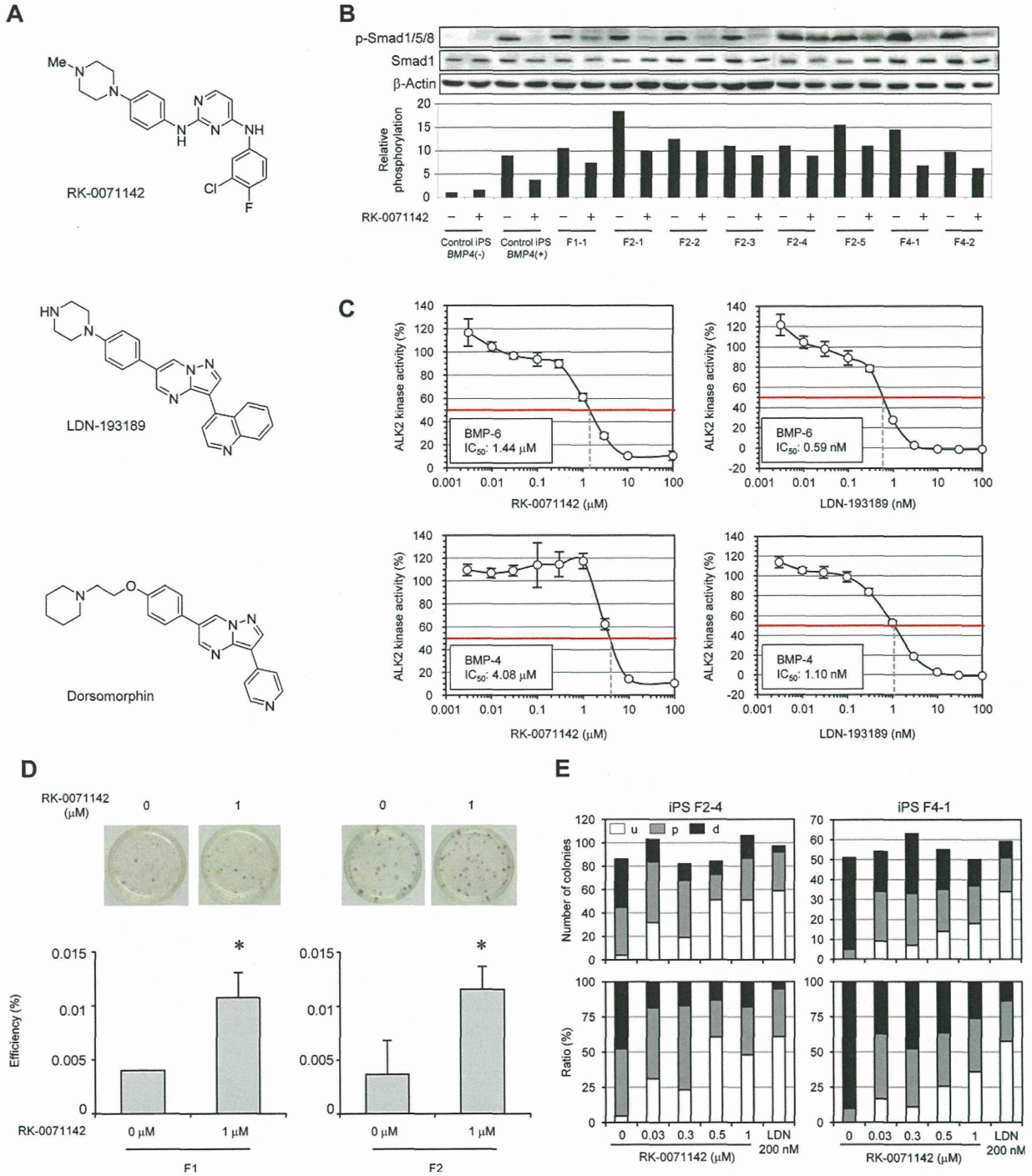

Figure 7. Screening for new candidates as ALK2 inhibitors. **(A):** Structures of RK-0071142, LDN-193189, and Dorsomorphin. **(B):** Immunoblot analysis of p-Smad1/5/8 and total Smad1 in fibrodysplasia ossificans progressive (FOP)-derived induced pluripotent stem (iPSC) lines with or without RK-0071142 treatment. RK-0071142 (1 μM) treatment suppressed the phosphorylation of Smad1/5/8. The relative phosphorylation level was normalized to the expression of Smad1 in each iPSC line. F1-1, F2-1, F2-2, F2-3, F2-4, F2-5, F4-1, and F4-2 are FOP-derived iPSC lines. Control iPSC line: Normal iPSC line. **(C):** Inhibitory activity of RK-0071142 and LDN-193189 for bone morphogenetic proteins (BMPs). The kinase activity of ALK2 was measured and determined by the promoter activity specific for ALK2 signals (supporting information Fig. S7). IC_{50} of bone morphogenetic protein-6 (BMP-6) (upper panel) and bone morphogenetic protein-4 (BMP-4) (lower panel) was calculated using a kinetic graph of ALK2 activity. **(D):** Alkaline phosphatase (AP)-staining of iPSC colonies from patient F1 and F2 in 60 mm dishes treated with or without RK-0071142 (top). Efficiency of formation of iPSC colonies in cultures treated with or without RK-0071142 (bottom). AP^+ colony with undifferentiated colony morphology was counted on day 30 of iPSC induction. The cultures were treated with RK-0071142 from day 8 to day 30 of the induction period. *, $p < .05$. **(E):** The number and ratio of the three types of colonies (described in Fig. 3A) in FOP-derived iPSC lines treated with RK-0071142 at various concentrations. Spontaneous differentiation of FOP-derived iPSC lines was suppressed by RK-0071142 treatment. The suppression intensity of RK-0071142 was similar to that of LDN-193189. Abbreviations: ALK2, activin receptor-like kinase 2; BMP, bone morphogenetic protein; LDN, LDN-193189.

generation of iPSCs, suggesting that enhancement of iPSC generation by BMP signaling is mediated by the receptor consisting of BMPRII and ALK3 [41]. Although these findings indicate that BMP signaling together with the receptors BMPRII and ALK3 are implicated in the generation of iPSCs, the role of other receptors, such as ALK2 and ALK6, in cellular reprogramming remains unknown. We show here that during the early phase of iPSC induction, from day 1 to day 7, treatment with an ALK2 inhibitor can suppress the generation of iPSCs from normal fibroblasts. Thus, BMP signaling mediated by ALK2 is necessary for reprogramming during the early phase of iPSC generation. In contrast to the previous findings for BMPRII and ALK3, we show here that constitutive activation of ALK2 affects both the upregulation of pluripotent markers and the downregulation of fibroblastic markers during the early phase of iPSC generation resulting in incomplete reprogramming. Signaling by BMP type I receptors appears to regulate iPSC generation through different mechanism; ALK3 signaling stimulated by BMPs can enhance the iPSC generation by promoting MET, whereas constitutive activation of ALK2 can suppress iPSC generation by reprogramming the pluripotent and fibroblastic markers insufficiently. The downstream molecules mediated by ALK2 are known to be similar but not identical to those mediated by ALK3. The BMP type I receptors, ALK2, 3, and 6, act as downstream components of type II receptors and phosphorylate Smad proteins [42, 43]. Whereas ALK3 and ALK6 phosphorylates Smad1, 5, and 8, ALK2 only phosphorylates Smad1 and 5 under physiological conditions [44]. In addition, ALK3 signaling has a functionally different effect from that of ALK2 and 6 on cellular apoptosis of hippocampal progenitors [45]. These studies can support our results that the effect of ALK2 on iPSC generation is different from that of ALK3.

We demonstrated that constitutive activation of ALK2 repressed the formation of iPSC colonies due to the forced differentiation of the cells during and after reprogramming. Consistently, LDN treatment at later stages of iPSC generation (from day 8 to day 30) restored the colony-forming capacity of FOP-derived iPSCs. Therefore, the molecular basis of the inhibitory effect on colony formation is the same as that causing repression of iPSC generation from FOP fibroblasts. BMP signaling is known to be important for maintaining the pluripotency of mouse ESCs. Mouse ESCs can be continuously cultivated with BMP-4 in the presence of leukemia inhibiting factor under serum-free conditions [46]. In contrast, in human ESCs and mouse epiblast stem cell studies, BMP-4 has been shown to induce trophoblastic lineage [47] as well as germ cell lineage differentiations [48]. In human ESCs, BMP-4 together with FGF2 can switch the cell lineage outcome to mesendoderm [49]. We demonstrated here that constitutive activation of ALK2 in the presence of FGF2 is forced to induce differentiation into both mesoderm and endoderm. This result suggests that BMP signaling mediated by ALK2 can synergy with FGF2 to direct iPSCs into both mesodermal and endodermal cells.

Several recent studies have reported that iPSCs established from patients can not only recapitulate some aspects of diseases but also can be used to better design and anticipate results from translational medicine [12–16]. Our study demonstrates that the aberrant molecular events occurring in diseases can impair the generation of iPSCs and that by restoring these events the efficiency of iPSC generation can also be restored. Thus, investigations into why iPSC production in diseases is inhibited can help unravel the underlying molecular and pathogenic events of these diseases.

This study also highlights the inefficient production of iPSCs as a useful disease phenotype not only for studying the molecular mechanisms underlying iPS reprogramming but also for identifying drug candidates for future therapies. In addition to the other ways to select drug candidates such as the measurement of kinase activity, the reprogramming process serves well as a validation tool for specific application. Although the system used here did not appear to be relevant to the symptoms of FOP, we showed that LDN, a known inhibitor of ALK2, could improve the efficiency of both the generation and the maintenance of iPSCs derived from FOP patients. In combination with in silico chemical library screening, we screened a chemical library to identify candidates with the ability to restore iPSC induction in FOP-derived fibroblasts. Using this approach, we identified a new ALK2 inhibitor candidate, RK-0071142, with potential for future therapeutic applications in the treatment of FOP. Since constitutive activation of ALK2 plays a pivotal role in the pathogenesis of FOP, screening for and evaluating new compounds as ALK2 inhibitors is expected to be the first step toward developing new drugs for the treatment of FOP. The patient-derived cellular model presented here has the potential to not only lead to the discovery of new compounds to treat FOP but also to be applied as a strategy to develop future therapies for other human diseases.

Acknowledgments

We would like to thank Masaki Takahashi for technical support, and Dr. Yuki Yanagihara and Dr. Kohei Miyazono for providing materials and helpful discussion. We also thank RIKEN Program for Drug Discovery and Medical Technology Platforms for providing the chemical compounds. This study was supported in part by grants from the Ministry of Health, Labor, and Welfare of Japan and Core Research for Evolutional Science and Technology (CREST), Japan Science and Technology Agency.

Disclosure of Potential Conflicts of Interest

The authors indicate no potential conflicts of interest.

References

1 Kaplan FS, Seemann P, Haupt J et al. Investigations of activated ACVR1/ALK2, a bone morphogenetic protein type I receptor, that causes fibrodysplasia ossificans progressiva. Methods Enzymol 2010; 484:357–373.

2 Shore EM, Kaplan FS. Insights from a rare genetic disorder of extraskeletal bone formation, fibrodysplasia ossificans progressiva (FOP). Bone 2008;43:427–433.

3 Fukuda T, Kohda M, Kanomata K et al. Constitutively activated ALK2 and increased SMAD1/5 cooperatively induce bone morphogenetic protein signaling in fibrodysplasia ossificans progressiva. J Biol Chem 2009;284:7149–7156.

4 Billings PC, Fiori JL, Bentwood JL et al. Dysregulated BMP signaling and enhanced osteogenic differentiation of connective tissue progenitor cells from patients with fibrodysplasia ossificans progressiva (FOP). J Bone Miner Res 2008;23:305–313.

5 Fiori JL, Billings PC, de la Pena LS et al. Dysregulation of the BMP-p38 MAPK signaling pathway in cells from patients with fibrodysplasia ossificans progressiva (FOP). J Bone Miner Res 2006;21:902–909.

6 Kaplan FS, Xu M, Seemann P et al. Classic and atypical fibrodysplasia ossificans progressiva (FOP) phenotypes are caused by mutations in the bone morphogenetic protein (BMP) type I receptor ACVR1. Hum Mutat 2009;30:379–390.
7 Shafritz AB, Shore EM, Gannon FH et al. Overexpression of an osteogenic morphogen in fibrodysplasia ossificans progressiva. N Engl J Med 1996;335:555–561.
8 Shen Q, Little SC, Xu M et al. The fibrodysplasia ossificans progressiva R206H ACVR1 mutation activates BMP-independent chondrogenesis and zebrafish embryo ventralization. J Clin Invest 2009;119: 3462–3472.
9 Shore EM, Xu M, Feldman GJ et al. A recurrent mutation in the BMP type I receptor ACVR1 causes inherited and sporadic fibrodysplasia ossificans progressiva. Nat Genet 2006;38:525–527.
10 Furuya H, Ikezoe K, Wang L et al. A unique case of fibrodysplasia ossificans progressiva with an ACVR1 mutation, G356D, other than the common mutation (R206H). Am J Med Genet A 2008;146A: 459–463.
11 Fukuda T, Kanomata K, Nojima J et al. A unique mutation of ALK2, G356D, found in a patient with fibrodysplasia ossificans progressiva is a moderately activated BMP type i receptor. Biochem Biophys Res Commun 2008;377:905–909.
12 Dimos JT, Rodolfa KT, Niakan KK et al. Induced pluripotent stem cells generated from patients with ALS can be differentiated into motor neurons. Science 2008;321:1218–1221.
13 Ebert AD, Yu J, Rose FF, Jr. et al. Induced pluripotent stem cells from a spinal muscular atrophy patient. Nature 2009;457:277–280.
14 Liu GH, Barkho BZ, Ruiz S et al. Recapitulation of premature ageing with iPSCs from Hutchinson-Gilford progeria syndrome. Nature 2011; 472:221–225.
15 Marchetto MC, Carromeu C, Acab A et al. A model for neural development and treatment of Rett syndrome using human induced pluripotent stem cells. Cell 2010;143:527–539.
16 Soldner F, Hockemeyer D, Beard C et al. Parkinson's disease patient-derived induced pluripotent stem cells free of viral reprogramming factors. Cell 2009;136:964–977.
17 Takahashi K, Yamanaka S. Induction of pluripotent stem cells from mouse embryonic and adult fibroblast cultures by defined factors. Cell 2006;126:663–676.
18 Takahashi K, Tanabe K, Ohnuki M et al. Induction of pluripotent stem cells from adult human fibroblasts by defined factors. Cell 2007; 131:861–872.
19 Itzhaki I, Maizels L, Huber I et al. Modelling the long QT syndrome with induced pluripotent stem cells. Nature 2011;471:225–229.
20 Koch P, Breuer P, Peitz M et al. Excitation-induced ataxin-3 aggregation in neurons from patients with Machado-Joseph disease. Nature 2011;480:543–546.
21 Yazawa M, Hsueh B, Jia X et al. Using induced pluripotent stem cells to investigate cardiac phenotypes in Timothy syndrome. Nature 2011; 471:230–234.
22 Hong H, Takahashi K, Ichisaka T et al. Suppression of induced pluripotent stem cell generation by the p53-p21 pathway. Nature 2009;460: 1132–1135.
23 Li H, Collado M, Villasante A et al. The Ink4/Arf locus is a barrier for iPS cell reprogramming. Nature 2009;460:1136–1139.
24 Fusaki N, Ban H, Nishiyama A et al. Efficient induction of transgene-free human pluripotent stem cells using a vector based on Sendai virus, an RNA virus that does not integrate into the host genome. Proc Jpn Acad Ser B Phys Biol Sci 2009;85:348–362.
25 Seki T, Yuasa S, Oda M et al. Generation of induced pluripotent stem cells from human terminally differentiated circulating T cells. Cell Stem Cell 2010;7:11–14.
26 Ban H, Nishishita N, Fusaki N et al. Efficient generation of transgene-free human induced pluripotent stem cells (iPSCs) by temperature-sensitive Sendai virus vectors. Proc Natl Acad Sci USA 2011;108: 14234–14239.
27 Yu PB, Deng DY, Lai CS et al. BMP type I receptor inhibition reduces heterotopic [corrected] ossification. Nat Med 2008;14: 1363–1369.
28 Cuny GD, Yu PB, Laha JK et al. Structure-activity relationship study of bone morphogenetic protein (BMP) signaling inhibitors. Bioorg Med Chem Lett 2008;18:4388–4392.
29 Tada S, Era T, Furusawa C et al. Characterization of mesendoderm: A diverging point of the definitive endoderm and mesoderm in embryonic stem cell differentiation culture. Development 2005;132: 4363–4374.
30 Sakurai H, Era T, Jakt LM et al. In vitro modeling of paraxial and lateral mesoderm differentiation reveals early reversibility. Stem Cells 2006;24:575–586.
31 Niwa H, Toyooka Y, Shimosato D et al. Interaction between Oct3/4 and Cdx2 determines trophectoderm differentiation. Cell 2005;123: 917–929.
32 Takashima Y, Era T, Nakao K et al. Neuroepithelial cells supply an initial transient wave of MSC differentiation. Cell 2007;129: 1377–1388.
33 Niwa H, Miyazaki J, Smith AG. Quantitative expression of Oct-3/4 defines differentiation, dedifferentiation or self-renewal of ES cells. Nat Genet 2000;24:372–376.
34 Mitsui K, Tokuzawa Y, Itoh H et al. The homeoprotein Nanog is required for maintenance of pluripotency in mouse epiblast and ES cells. Cell 2003;113:631–642.
35 Chambers I, Colby D, Robertson M et al. Functional expression cloning of Nanog, a pluripotency sustaining factor in embryonic stem cells. Cell 2003;113:643–655.
36 Raychaudhuri S, Stuart JM, Altman RB. Principal components analysis to summarize microarray experiments: Application to sporulation *time series. Pac Symp Biocomput2000:455–466.*
37 Takahashi M, Katagiri T, Furuya H et al. Disease-causing allele-specific silencing against the ALK2 mutants, R206H and G356D, in fibrodysplasia ossificans progressive. Gene Ther 2012;19:781–785.
38 Ichida JK, Blanchard J, Lam K et al. A small-molecule inhibitor of tgf-Beta signaling replaces sox2 in reprogramming by inducing nanog. Cell Stem Cell 2009;5:491–503.
39 Attisano L, Carcamo J, Ventura F et al. Identification of human activin and TGF beta type I receptors that form heteromeric kinase complexes with type II receptors. Cell 1993;75:671–680.
40 Maherali N, Hochedlinger K. Tgfbeta signal inhibition cooperates in the induction of iPSCs and replaces Sox2 and cMyc. Curr Biol 2009; 19:1718–1723.
41 Samavarchi-Tehrani P, Golipour A, David L et al. Functional genomics reveals a BMP-driven mesenchymal-to-epithelial transition in the initiation of somatic cell reprogramming. Cell Stem Cell 2010; 7:64–77.
42 Balemans W, Van Hul W. Extracellular regulation of BMP signaling in vertebrates: A cocktail of modulators. Dev Biol 2002;250:231–250.
43 Watabe T, Miyazono K. Roles of TGF-beta family signaling in stem cell renewal and differentiation. Cell Res 2009;19:103–115.
44 Aoki H, Fujii M, Imamura T et al. Synergistic effects of different bone morphogenetic protein type I receptors on alkaline phosphatase induction. J Cell Sci 2001;114:1483–1489.
45 Brederlau A, Faigle R, Elmi M et al. The bone morphogenetic protein type Ib receptor is a major mediator of glial differentiation and cell survival in adult hippocampal progenitor cell culture. Mol Biol Cell 2004;15:3863–3875.
46 Ying QL, Nichols J, Chambers I et al. BMP induction of Id proteins suppresses differentiation and sustains embryonic stem cell self-renewal in collaboration with STAT3. Cell 2003;115:281–292.
47 Xu RH, Chen X, Li DS et al. BMP4 initiates human embryonic stem cell differentiation to trophoblast. Nat Biotechnol 2002;20:1261–1264.
48 West FD, Roche-Rios MI, Abraham S et al. KIT ligand and bone morphogenetic protein signaling enhances human embryonic stem cell to germ-like cell differentiation. Hum Reprod 2010;25:168–178.
49 Yu P, Pan G, Yu J et al. FGF2 sustains NANOG and switches the outcome of BMP4-induced human embryonic stem cell differentiation. Cell Stem Cell 2011;8:326–334.

See www.StemCells.com for supporting information available online.

ARTICLE

Facial morphology and occlusion of a patient with fibrodysplasia ossificans progressiva (FOP): a case report

Takafumi Susami, DDS, PhD;[1]* Yoshiyuki Mori, DDS, PhD;[1] Kazumi Tamura;[2] Kazumi Ohkubo, DDS, PhD;[3] Kouhei Nagahama, DDS, PhD;[4] Naoko Takahashi, DDS;[4] Natsuko Uchino, DDS;[4] Kiwako Uwatoko, DDS;[4] Nobuhiko Haga, MD, PhD;[5] Tsuyoshi Takato, MD, PhD[6]

[1]Associate Professor; [2]Oral Hygienist; [3]Assistant Professor; [4]Orthodontist—Department of Oral-Maxillofacial Surgery, Dentistry and Orthodontics; [5]Professor, Department of Rehabilitation Medicine; [6]Professor, Department of Oral-Maxillofacial Surgery, Dentistry and Orthodontics—The University of Tokyo Hospital, Tokyo, Japan.
*Corresponding author e-mail: susami-ora@h.u-tokyo.ac.jp

Spec Care Dentist 32(4): 165-170, 2012

ABSTRACT

Fibrodysplasia ossificans progressiva (FOP) is a rare disease characterized by postnatal heterotopic ossification (HO). When HO affects the masticatory muscles, mouth opening becomes restricted. This paper presents the changes in facial morphology and occlusion of a patient with FOP who was followed from the age of 8 to age 21. At the initial examination, he had a severely protruded maxilla and Angle Class II Division 1 malocclusion. His mouth opening was restricted (5.0 mm). He had a large overjet and this enabled him to clean his teeth and to eat. Orthodontic correction was not planned, and his facial growth was closely followed with attention to his oral hygiene. The maxillary protrusion and a low mandibular plane angle became more prominent as the patient aged. His mandible rotated in a counterclockwise direction. His molars had delayed eruption or were impacted and seven were extracted. His mouth opening increased slightly and his oral hygiene improved to excellent.

KEY WORDS: fibrodysplasia ossificans progressiva (FOP), heterotopic ossification, facial morphology, occlusion, growth

Introduction

Fibrodysplasia ossificans progressiva (FOP) is an autosomal dominant disorder characterized by postnatal heterotopic ossification (HO).[1,2] The disorder is caused by a gene mutation in the activin A receptor type I (ACVR1), which is responsible for bone morphogenetic protein (BMP) activity.[3,4] The incidence of FOP is quite rare, affecting an estimated one in 2 million people. HO is usually not apparent at birth; congenital malformation of the great toes is a sign for early diagnosis of the disorder. HO often appears within the first decade of life, after swelling with sensation of heat and pain (flare-up) of the soft tissues such as the skeletal muscles, tendons, and ligaments. When HO occurs in tissues surrounding joints, their mobility is lost.[1,2,5-7] In the maxillofacial region, the temporomandibular joint (TMJ) and masticatory muscles are common sites of involvement and this results in restricted mouth opening.[5,8-14] Surgical treatment for the restricted mouth opening in patients with FOP often results in relapse and worsening of HO and is generally not recommended.[1,15-18] HO in growing children affects facial growth and occlusion. Although there are a few reports about occlusion,[19,20] little is known about the facial morphology and occlusion of patients with FOP. In this paper, we present a longitudinal record of facial morphology and occlusion (from 8 to 21 years of age) in a patient with FOP, and discuss the dental care for children with FOP.

Case report

The patient first visited the University of Tokyo Hospital at the age of 8 years and 9 months. He had severe maxillary protrusion in the mixed dentition with a large overjet (9.5 mm) and a deep overbite (5.0 mm). The molar relationship was Angle Class II (Angle Classification Class II, Division 1). His mouth opening was severely restricted and the maximum opening was 5.0 mm (Figure 1). Evaluation of the patient's panoramic radiograph revealed the presence of all permanent teeth, widening of the right coronoid process, and elongation of the left coronoid process; mild flattening of the bilateral condylar heads was suspected

doi: 10.1111/j.1754-4505.2012.00260.x

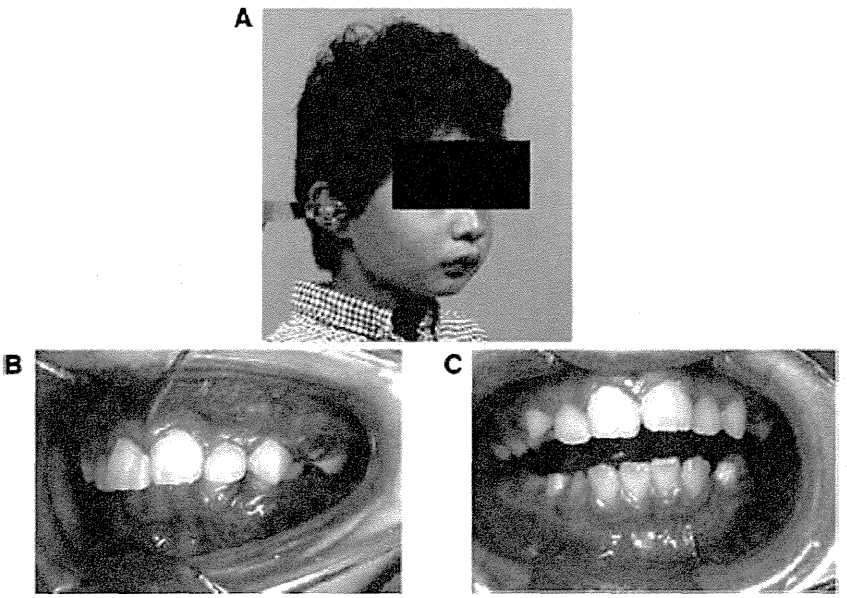

Figure 1. Facial appearance and occlusion at the initial visit (age 8 years, 9 months). (A) Face. (B) Occlusion at closed position. (C) Maximum opening. The occlusion showed severe maxillary protrusion and the amount of maximum mouth opening was 5.0 mm.

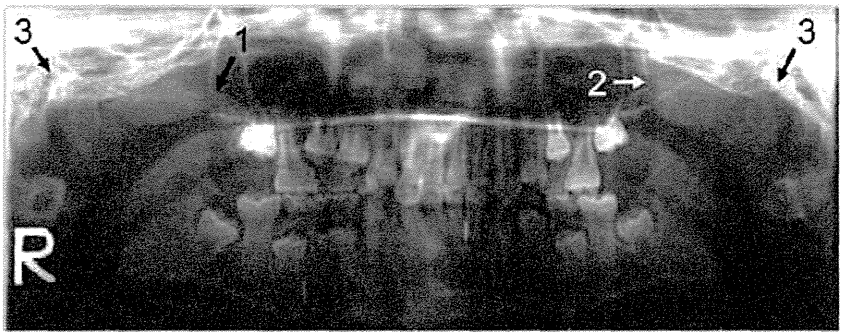

Figure 2. Panoramic radiograph at the initial visit (age 8 years, 9 months). Widening of the right coronoid process (arrow 1) and elongation of the left coronoid process (arrow 2) were seen. Mild flattening of the bilateral condylar heads was suspected (arrows 3).

(Figure 2). The lateral cephalogram showed a severe Class II facial skeleton (SNA: 85.4°, SNB: 75.6°, ANB: 9.8°) (Figure 3, Table 1). The maxilla was protruded and the mandible had normal anteroposterior development. Both maxillary and mandibular incisors were proclined and fusion of cervical vertebrae was also noted in the cephalogram. At that time, the spinal deformity in the coronal plane (scoliosis) was mild (Figure 4A).

The patient had received surgical correction of bilateral hallux valgus at the age of 1 year and was diagnosed with FOP in another hospital at 5 years of age. As the large overjet enabled his teeth to be cleaned and for him to eat, orthodontic correction was not planned and it was decided to follow his facial growth carefully and to maintain his oral hygiene at the highest level.

At 12 years of age, the patient had pain in his right hip joint, which affected his movement. From 13 years of age, HO in the ligaments surrounding the vertebral column progressed, and scoliosis and tilting of the head became more prominent (Figures 4B and 5). At 16 years of age, the last cephalogram was made; as it was impossible thereafter because of his vertebral deformation. The superimposition of cephalogram tracings at ages 8 and 16 showed greater forward growth of both the maxilla and mandible relative to the anterior cranial base. The mandible showed counterclockwise rotation and both maxillary and mandibular incisors were proclined further (Figure 6, Table 1). The computed tomography (CT) made at 16 years of age clearly depicted deformation of bilateral condylar heads, widening of the right coronoid process, and elongation of the left coronoid process. HO was found at the anterior edge of the right coronoid process, but it was not fused with the upper bones of the skull (Figure 7). These findings suggested that the restricted mouth opening was caused by the mechanical interference between the coronoid processes and upper bones, and not because there was a bony fusion. Between 16 and 17 years of age, the patient experienced acute

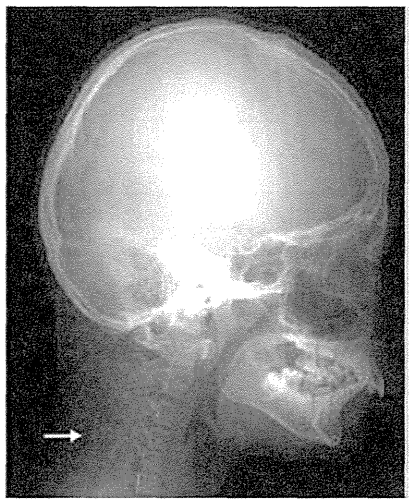

Figure 3. Lateral cephalogram at the initial visit (age 8 years, 9 months). The patient had severe Angle Class II facial skeleton. Fusion of cervical vertebrae was seen (arrow).

Table 1. Cephalogram measurements.

Parameters	Age		Japanese adult male norm:
	8 years, 10 months	16 years, 4 months	Mean (SD)
SNA	85.4[a]	93.5[c]	81.8 (3.1)
SNB	75.6	81.4	78.6 (3.1)
ANB	9.8[b]	12.1[c]	3.3 (2.7)
MP-FH	19.6[a]	11.8[b]	26.3 (6.3)
U1-FH	117.9[a]	126.4[c]	108.9 (5.6)
L1-MP	123.3[c]	129.5[c]	94.7 (7.2)

MP-FH: Mandibular plane–Frankfurt plane Angle; U1-FH: Upper incisor–Frankfurt plane Aznqle; L1-MP: Lower incisor-Frankfurt plane Angle; SD: Standard deviation.
Deviation from the mean value [a]between 1 and 2 SD, [b]between 2 and 3 SD, [c]more than 3 SD.
Japanese norm is from Izuka and Ishikawa[25]

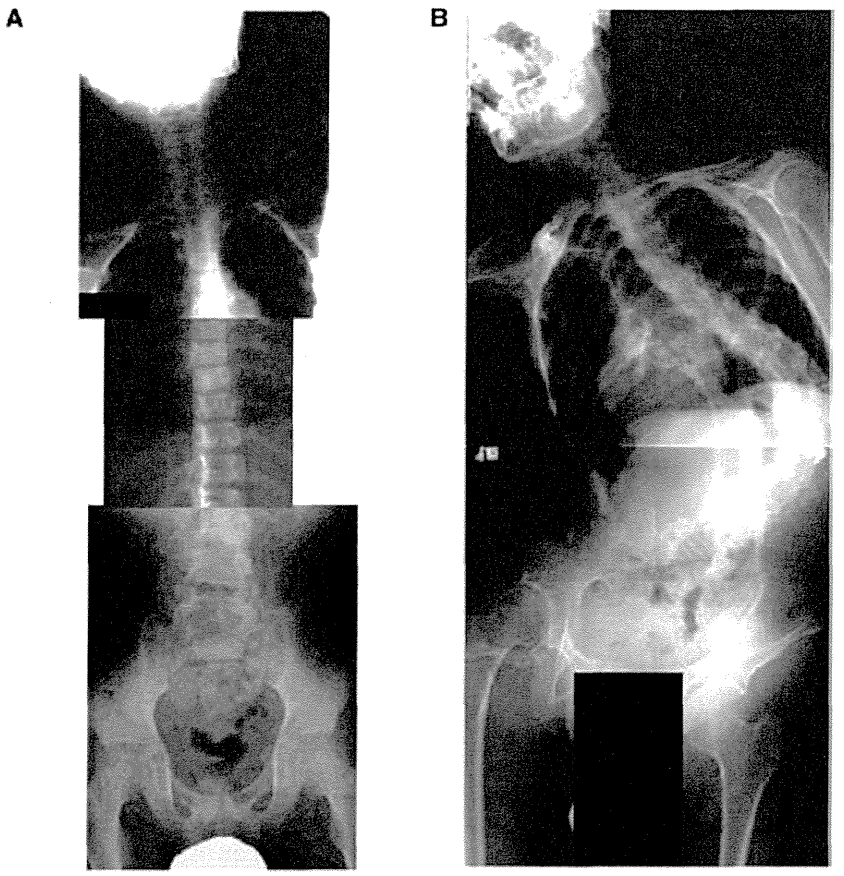

Figure 4. Integrated radiographic films of the vertebral column. (A) At the initial visit (age 8 years, 9 months). (B) At 18 years and 3 months of age, lateral curvature of the vertebral column had become severe.

Figure 5. Facial appearance at age 15 years and 4 months. Tilting of the head had become prominent and standardization using ear rods was impossible.

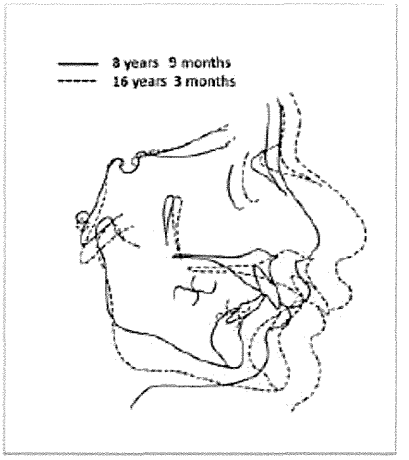

Figure 6. Superimposition of lateral cephalograms. Large forward growths of both maxilla and mandible were found. The mandible showed counterclockwise rotation and both maxillary and mandibular incisors were proclined further.

submandibular swelling (flare-up) twice and antibiotics and a bisphosphonate were administered. He also experienced swelling in the right elbow and forearm during that period.

At 19 years of age, the maxillary protrusion had increased. The overjet and overbite had increased to 12.0 and